Investigation of laminar forced convection using a different shape of a heat sink

Hiba K. Mohsen and *Naseer Hamza*

Mechanical Engineering Department, College of Engineering, University of Al-Qadisiyah , Al-Diwaniyah, 58001, Iraq.

A R T I C L E I N F O

A B S T R A C T

Improving the thermal design of geometric Heat Sinks (HSs) reduces their size and weight and improves heat dissipation, hence enhancing the speed of electronic devices. In this numerical study, a novel thermal design of HSs is proposed by inserting various forms in order to obtain the optimum thermal design for this type of HSs. This study has two primary objectives: determining the influence of varying types of HSs while maintaining the volume of fins, and introducing new geometries such as circular fin and circular cut fin. The tests were conducted with a heat flux of 11.1 kW/m2 and a Reynolds number (Re) ranging from 2418.56 to 819.19. For forced convection, three-dimensional numerical simulations utilising the Navier–Stokes equations laminar model and energy equation are acquired using the commercially available COMSOL Multi-physics version 5.6a CFD software. The results indicate that. A comparison analysis of HSs with different geometries revealed that the circular-cut shape exhibited the highest thermal efficiency, as measured by the Nusselt number about 153 as well as the heat transfer coefficient and the minimum thermal resistance.

1. Introduction

Heat sinks are a sort of heat exchanger that is created and used as a cooling system in electronic equipment such as processing units, and electronic components[1]. Several manufacturers have created compact, high-performing electronic devices in response to the modern electronic technology industry's ongoing growth. Under the conditions of excessive heat generation and the restrictions placed on the heat transfer area, the operating temperature may rise above the permissible range, which may cause the mechanism of the electronic device to malfunction. The right air-cooling system design is essential for ensuring the dependable operation and long lifespan of advanced electronic devices. The impact of geometry parameters on the ideal heat sink conditions has been the subject of

numerous research studies in the past. For instance, Elmi et al. [2] improved the tapered ratio of a Pin Fin Heat Sink (PFHS). It has been demonstrated that changing the fin design significantly impacts heat transfer and pressure drop. Furthermore, the overall performance of the pin fin heat sink improves by more than 17% during the optimization process. The heat transmission characteristics of PFHS at various fin types were demonstrated. Chingulpitak et al. [3] presented an analysis of the heat transfers and flow processes that occur when airflow is directed through crosscut heat sinks. Huang and Chen [4],[5] decreased the thermal resistance of the fin array by optimizing the thermal design of non-uniform fin widths of the heat sink. Their numerical and experimental results demonstrated that the thermal resistance decrease at Re = 5000 was approximately 12.7%, while Nu enhanced by approximately 14.5% compared to the original heat sink.

Nomenclature:

Ahs	Area of heat sinks (m^2)		*Greek symbols*	
Dh	Hydraulic diameter (m)		α	thermal diffusivity ($m^2\ s^{-1}$)
kf	thermal conductivity of the fluid (W m^{-1} K^{-1})		β	thermal expansion coefficient (K^{-1})
ks	thermal conductivity of solid (W m^{-1} K^{-1})		ρ	Density
hav	The average coefficient of heat transfer (W/m².K)		μ	dynamic viscosity (kg $m^{-1}s^{-1}$)
Nu	average Nusselt number			
p	pressure (kg $m^{-1}\ s^{-2}$)		*Subscripts*	
Re	Reynold number			
Pr	Prandtl number		SCFs	straight continuous fins
Ra	Rayleigh number		SCSPFs	straight continuous with square pin fins
$T_{a,\ mean}$	The temperature of air (°C)		SPFs	square pin fins
$T_{b,\ mean}$	Base temperature of heat sinks (°C)			
Q	Heat transfer rate (watt)			
P_{ch}	the perimeter of the minimum airflow channel		CFs	circular fins
u	Velocity in x-direction (m/s)			
v	Velocity in y-direction (m/s)		CCFs	circular cut fins
z	Velocity in z-direction (m/s)			
$\overset{\cdot}{m}$	Mass flow rate (kg/s)			

The effects of the crosscut length, the number of crosscuts, and the Re were investigated, and thermal resistance and pressure were measured as a result. An additional feature that was demonstrated was a flow visualization of the air that was contained within the crosscut heat sink. According to what they stated, the optimal ratio of thermal resistance could be achieved if the crosscut length was somewhere between 1.5 and 2.0 mm. The thermal performance of triangular fins, both with and without longitudinal perforations, was significantly improved by Shadlaghani et al. [6]. When testing was done, it was discovered that a fin with a triangular cross-section allowed for the greatest amount of convection heat transfer, followed by fins with rectangular and trapezoidal cross-sections. When the height/thickness ratio was increased, triangular fins were able to achieve the highest possible level of heat transfer enhancement. Experimentally, Nilpueng et al.[7] increased the heat convection of heat sinks made of sinusoidal wavy plate-fins and cross-cut sinusoidal wavy plate-fins. It was found that altering the flow velocity and shift stage facilitated the thermal transition and pressure decline. Furthermore, the sinusoidal wavy plate-fin has a greater Nusselt number ranging from 5.9 to 19.1%. Freegah et al.[8] created a new thermal prototype for plate-fin heat sinks using computational methods. Finned heat sinks without fillet, with fillet, with fillet profile by creating symmetrical half-round pins in vertical framework, ribbed half-round pins through perpendicular configuration, symmetrical half-round pins through parallel layout, and corrugated half-round pins through parallel arrangement were investigated. They stated that the decrease in base temperature, as well as thermal resistance of plate-fin heat, sinks with corrugated half-round pins arranged vertically and exposed to flow rate was roughly 25.1% and 29.0%, respectively, especially in comparison to plate-fins with a fillet profile, as well as a 34.48 percent rise in Nusselt number. Sertkaya et al. [9] conducted an experimental investigation of pin fin, plate, and finless plate heat sinks to optimize free convection heat transfer. The researchers altered the amount, height, distance, and direction of pin fins. It utilized 8 circular shaped pin fins as well as plate heat sinks with pin fin heights of 30 to 45 mm and pin fin diameters of 6 mm with three different directions of 0 °, 90 °and 180 °. The input power varied between 0 and 120 W, and the Rayleigh number varied between 1×10^6 and 7×10^6. It was discovered that 121×40 pin fin and plate heat sinks increased heat flow at all direction angles. Upon determining plate position, upward-facing heat sinks with a 0 °orientation angle value attained the highest heat transfer, whereas bottom heat sinks with a 180 °direction angle value attained the lowest. Altun and Ziylan [10] investigated the natural convection heat transfer in vertical sinusoidally wavy fins oriented horizontally. In this investigation, the length of the fin was fixed while the configuration of the fin was altered from rectangular to wavy, resulting in a range of new amplitude values. Experiments were conducted with wavy fins of three various amplitudes, H/30, H/15, and H/10, and varied heater power sources tend to range from 1.02W to 32.06W. The H/30, H/15, and H/10 values represent the H-values. According to the findings, wavy fins were more effective at improving heat transmission than rectangular fins. However, after a specific wave amplitude value, the increase in amplitude negatively impacts natural convection due to the obstruction of fluid movement because the higher amplitude causes the fluid to move more slowly. Feng et al. [11] conducted experimental and analytical research to enhance free convection heat transfer using a new prototype heat sink. A cross-fin heat sink with several long fins and short fins arranged orthogonally was proposed. They discovered that cross-fin heat sinks improved heat transfer characteristics by 15 percent more than plate-fin heat sinks. Furthermore, the enhancement was implemented without significantly increasing total volume, material consumption, or expense. Pathak et al. [12] numerically analyzed heat sink height's impact on thermal properties. According to the results, the variation of the average Nusselt number concerning the flow direction is more significant for nondimensional variable height heat sinks with limited fin spacing and a variable height of 0.25. When comparing fins with finite conductivities of 200 W/m-K and 75 W/m-K to an isothermal fin, the total Nusselt number is reduced by 5.7% and 9.5%, respectively. Using variable-height heat sinks in conjunction with a reduced fin height of 0.03 m, on the other hand, increases thermal efficiency by 225 percent. Moradikazerouni et al. [13] examined the thermal performance of a flat plate heat sink cooled by air through forced convection. The length of the fins was 60 mm, the Reynolds number was increased from 3.80 ×10^3 to

2.20 ×10^4, and the bottom of the heat sink was provided with 1000 W of power. They discovered that increasing the number and length of fins decreases the surface temperature of the plate by 25% and 20%, respectively. Yousfi et al. [14] analyzed the characteristics of forced convection in a pin fin heat sink. They computed the influence of the pyramid ratio on heat transfer and fluid flow characteristics. The Reynolds number varied between 8547 and 21367, and the pyramid ratio ranged from 0 to 1. The results indicated that the shape of pyramidal pin fins with a ratio of 1 provided the greatest improvement in hydrothermal performance. Tariq et al. [15] studied numerically and experimentally the advantages of plate-fin heat sinks with various perforations and slots. The new design of their flat-fin heat sinks has been determined to increase convection cooling and reduce pressure drop. Nusselt numbers for perforations and slots plate-fin heat sinks were 42.8% and 35.9%, respectively, for Re numbers 13049 to 52195. Using numerical methods, Razavi et al. [16] investigated the effect of heat sinks with splitter pin fins on forced convection. The profit factor's non-dimensional element (J) was calculated to account for both heat resistance and pressure drop effects. When the splitter length to pin diameter ratio L/D was increased, the pressure drop and heat resistance lowered while raising the profit factor. Usman et al. [17] carried out experimental research on paraffin wax, RT-44, and used RT-35HC containing triangular geometry heat sinks of 64 pin-fins with volume fractions of 9 percent and PCMs of 90 percent. The total heat output ranged from 5 to 8 watts. They reported that the triangular inline pin-fin is the most effective and requires the least amount of CPU. As passive cooling (RT-44), PCM yielded the most significant improvement. Bahiraei et al. [18] studied a heat sink's hydraulic and thermal performance with mini circular, triangular, and drop-shaped pin fins fabricated using green graphene nanofluid as the coolant. The results indicated that the thermal performance of the circular fins was superior to that of the triangular and drop-shaped pin fins. In addition, the thermal resistance decreased by 3.36 percent as the concentration rose from 0.025 percent to 0.075 percent. In addition, adding nanoparticles to the water did not affect the heat sink's pumping capacity.

Alhusseny et al. [19] performed numerical research on graphitic foam heat sinks to develop convective heat transfer. The heat sinks were constructed of staggered foam baffles placed perpendicularly or parallel to the coolant stream to reduce pressure loss while maintaining high thermal dissipation. It was discovered that the suggested heat sinks were effective enough to meet high-performance electronics' excessive thermal requirements and could also dissipate heat with acceptable pressure losses. It was indicated that the proper design parameters were applied in consideration of the operating parameters, thereby preventing the formation of any hot zones. Jilted et al. [20] presented the thermal performance of a concentric channel heat sink with an alternate slot for fluid flow analytically. Four concentric channels width 4 mm, depth 3.5 mm and parallel flow pathways were used to construct the heat sink slot spacing of 3 mm. At the base of the heat sink, a constant heat flux of 50 W and 70 W was applied, and nanoparticles had volume fractions ranging from 0.5 percent to 5 percent, with water as a standard fluid at a flow rate of 30 to 180 mL/min considered. The nanofluid-cooled heat sink demonstrated a higher rate of heat rejection than water. The augmentation was 2% for nanofluids with a volume fraction of 0.5 percent and 17% for nanofluids with a volume fraction of 5%.

The primary objective of the research is to determine the optimal heat sink geometry to achieve the highest possible cooling performance. In that regard, the COMSOL version 5.6a Multi-physics CFD software was used to investigate five distinct fin geometries, including straight continuous fins (SCFs), straight continuous with square pin fins (SCSPFs), square pin fins (SPFs), circular fins (CFs), and circular-cut fins (CCFs).

2. Problem description

The three-dimensional steady state heat sink shown in Fig. 1 was simulated by using COMSOL Multi-physics version 5.6a CFD. Pre-Processing, Solver Execution, and Post-Processing are the three main phases of CFD estimations. During the pre-processing stage, the computational mesh is generated, and the resolved objectives are decided upon. In the second step, configuration, boundary conditions, and numerical models are set to activate the solver. Fluid flow characteristics and exhibit geometry are used to define the fins as aluminum. The solver keeps going until the meeting starts. As soon as the solver is complete, the results are examined and the post is prepared. In the analysis, a PC with "11th Gen Intel(R) Core (TM) i7-1165G7 @ 2.80GHz " was used. The force convection heat transfer was attained numerically using a horizontal open-type wind channel.
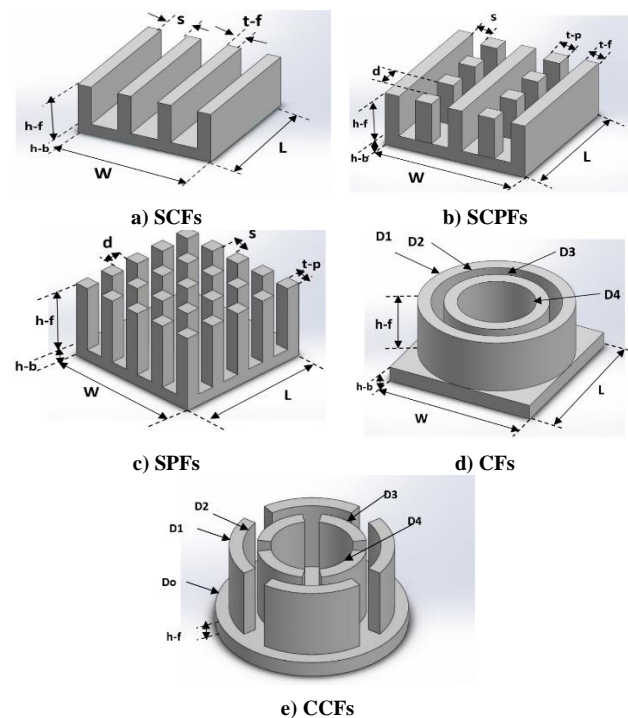

a) SCFs   **b) SCPFs**

c) SPFs   **d) CFs**

e) CCFs

Figure 1 Shows cases of study

The dimensions of the rectangular channel were 150 mm (width), 200 mm (height), and 800 mm (length) depicted in Fig. 2.

The middle part of the wind channel is contained of the heat sink, to ensure a fully developed flow entering the test section. The heat sink's bottom base is exposed to a constant heat flux. Thermal grease was utilised to improve heat transfer conduction between the surface of the plate heater and the bottom surface of the heat sink. The uniform air velocity at the inlet, air temperature of 26 C°, no-slip boundary conditions, and ambient pressure at the output have all been used.

Table 1. Dimensions of the cases study (mm)

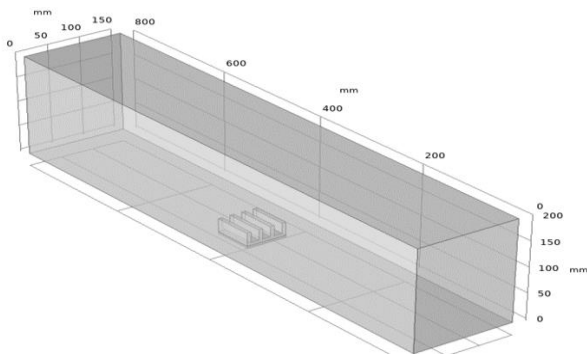| Case study	W	L	h-b	h-f	s	t-f	t-p	d	Dh
1.SCFs	60	60	6	20.6	12	6	-	-	15.17
2. SCSPFs	60	60	6	20.17	7	6	7	10.66	10.39
3. SPFs	60	60	6	33	7.5	6	6	7.5	12.22
Case study	W	L	h-b	h-f	D1	D2	D3	D4	Dh
4. CFs	60	60	6	21	60	50	40	30	10
5. CCFs	-	-	6	27	60	50	40	30	18

Figure 2. 3D computational domain the wind channel

Table 2 The average Nusselt number along SCFs using different mesh sizes.

Type of mesh	Number of nods	Average Nusselt number	Deviation in percentage
Extremely coarse	23532	69.84	
Extra Coarse	42855	70.69	1.22%
Coarser	82216	72.32	2.31%
Coarse	198995	74.71	3.30%
Normal	451946	75.56	1.14%
Fine	1336101	75.64	0.11%
Finer	3996683	75.81	0.22%

The numerical tests are performed on each type to ensure that solutions are independent of grid size based on comparisons of average Nusselt numbers as well as average temperature related to heat sinks. Table 2 shows, that the optimal mesh for SCFs in terms of accuracy and solution time is the normal grid of (451946). In Figure. 3. the mesh was bullied along the channel and case study.
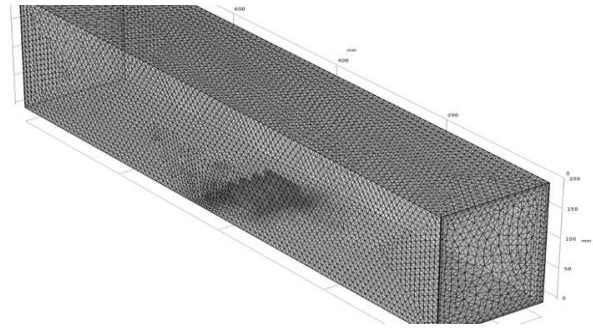

Figure 3. 3D computational quadratic mesh of the domain

3. Governing equations

The equations of Navier-Stokes are used as governing the forced convection fluid flow of the system. The following assumptions have been made:

1- The working fluid is air.

2- The flow is considered as a steady, continuum, fully developed, and three-dimensional.

3- The outside sides of the rectangular duct were insulated, except the heat sink base plate, for which a continuous heat flow emulating the electronic heater's heat production was required.

4- Material characteristics remained unchanged. Except for viscosity, fluid characteristics were temperature-independent.

5-Flow is considered laminar due to Re is less than 2500.

6-Negligible radiation heat transfer.

7-The thermophysical properties of air are considered to be constant.

For airflow:

Continuity equation:

$$\frac{\partial u}{\partial x} + \frac{\partial v}{\partial y} + \frac{\partial w}{\partial z} = 0 \qquad (1)$$

x- momentum equation:

$$u\frac{\partial u}{\partial x} + v\frac{\partial u}{\partial y} + w\frac{\partial u}{\partial z} = -\frac{1}{\rho_0}\frac{\partial p}{\partial x} + \vartheta\left(\frac{\partial^2 u}{\partial x^2} + \frac{\partial^2 u}{\partial y^2} + \frac{\partial^2 u}{\partial z^2}\right) \qquad (2)$$

y- momentum equation:

$$u\frac{\partial v}{\partial x} + v\frac{\partial v}{\partial y} + w\frac{\partial v}{\partial z} = -\frac{1}{\rho_0}\frac{\partial p}{\partial y} + \vartheta\left(\frac{\partial^2 v}{\partial x^2} + \frac{\partial^2 v}{\partial y^2} + \frac{\partial^2 v}{\partial z^2}\right) \qquad (3)$$

z- momentum equation:

$$u\frac{\partial w}{\partial z} + v\frac{\partial w}{\partial y} + w\frac{\partial w}{\partial z} = -\frac{1}{\rho_0}\frac{\partial p}{\partial x} + \vartheta\left(\frac{\partial^2 w}{\partial x^2} + \frac{\partial^2 w}{\partial y^2} + \frac{\partial^2 w}{\partial z^2}\right) \qquad (4)$$

Energy equation:

$$u\frac{\partial T}{\partial x} + v\frac{\partial T}{\partial y} + w\frac{\partial T}{\partial z} = \frac{K_f}{\rho_0 C_p}\left(\frac{\partial^2 T}{\partial x^2} + \frac{\partial^2 T}{\partial y^2} + \frac{\partial^2 T}{\partial z^2}\right) \qquad (5)$$

3.1 Dimensional governing equations in a heat sink

$$K_s\left(\frac{\partial^2 T}{\partial x^2} + \frac{\partial^2 T}{\partial y^2} + \frac{\partial^2 T}{\partial z^2}\right) + \dot{q}_s = 0 \qquad (6)$$

3.2 Domain and boundary conditions for computation: [21]

Inlet:

$$T = T_{in} = 298\,K, v = u = w = 0$$

Outlet:

$$p = p_{out} = 0, u = w = 0, \frac{\partial T}{\partial y} = 0$$

Adiabatic walls:

$$u = v = w = 0, \frac{\partial T}{\partial z} = \frac{\partial T}{\partial x} = 0$$

Heated wall:

$$u = v = w = 0, q_w'' = -k\frac{\partial T}{\partial x}$$

The rate of heat transfer from the heat sink was evaluated using:

$$Q = m_{\cdot a}C_{pa}(T_{out} - T_{in}) \qquad (7)$$

The overall heat transfer coefficient is determined by:

$$h_{av} = \frac{Q}{A_{hs}(T_{b,\,mean} - T_{a,\,mean})} \qquad (8)$$

The Nusselt number can be determined using the following formula:

$$N_u = \frac{h_{av}D_h}{k_a} \qquad (9)$$

Where:

$$D_h = 4\frac{A_f}{P_{ch}} \qquad (10)$$

The Reynolds number can be calculated from:

$$R_e = \frac{\rho_a V_{av} D_h}{\mu_a} \qquad (11)$$

The thermal Resistance can be determined from:

$$R_{th} = \frac{T_b - T_{in}}{Q}$$

4. Results and discussions

The present simulation models are first validated with the recent experimental results of Nilpueng et al.[1] that studied the effects of pin fin configuration on the thermal performance of plate pin fin heat sinks. They employed a duct that cross-section area of 675mm2 with a total length of 0.8 m. A uniform heat flux of about q $''$ = 14.81 kW/m^2 was applied to the bottom base of the heat sink. While the Reynolds number was studied within the range of (1100 to 3000). In this comparison, the heat transfer coefficient is compared with different Reynold numbers for SCFs as shown in **Figure 4**.

As previously stated, the computations have been performed at various Reynolds numbers for the five types of HS arrays. Furthermore, all of the data were obtained under steady-state settings. **Figures 5** provides contour plots of the surface temperature distributions for all heat sink shapes examined at 2.4 m/s velocities, and power input (40W). The figure depicts the maximum temperature occurring at the heated bottom wall concerning the heat sink because of the high thermal conductivity of aluminum. The best heat dissipation was substantial between models (d) and (e). The circular fin and circular cut show a good performance in the process of heat dissipation. The reason beyond that is the positive effect of the curvature of these configurations on the flow characteristics hydrodynamically and thermally. The curvature of the circular path of proposed extended surfaces enhances the flow velocity which in its turn increases the Reynolds number

and thus the Nusselt number and consequently increase the rate of heat dissipation, the matter which is examined later throughout this study Furthermore, the rapid heat dissipation to the environment due to the increased surface area exposed to air, increasing airflow.
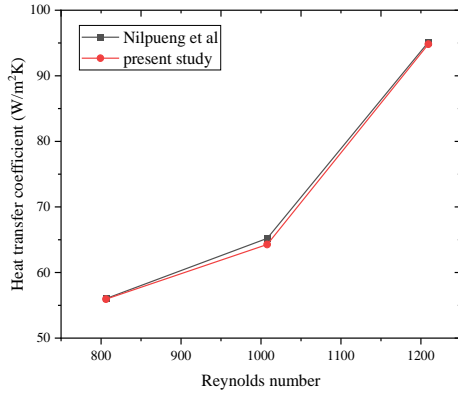
Figures 6 provide contour plots of the surface temperature distributions for all heat sink shapes at velocity 1.8m/s, and power input (40W). As a result of a reduction in convective heat transmission, the surface temperature rises.
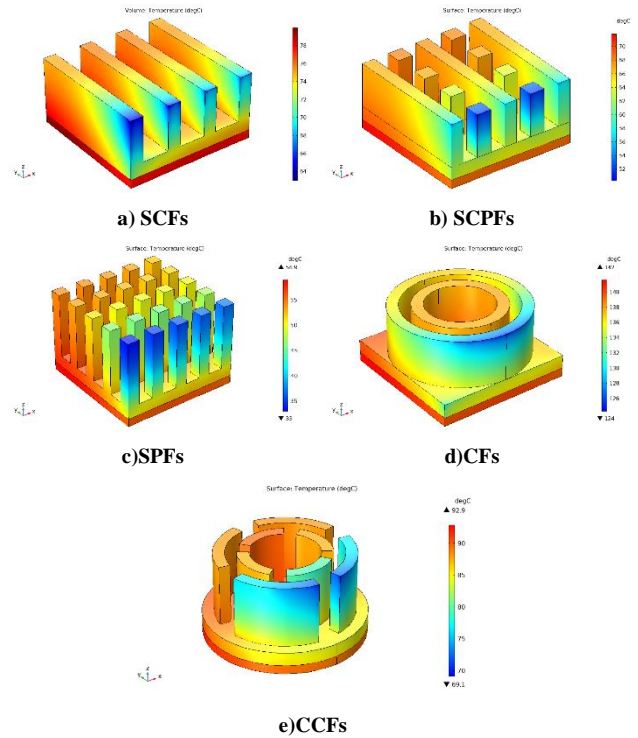

Figure 4 Comparison the heat transfer coefficient versus Re between the current work with those obtained by Nilpueng et al[1] at , q= 14.81kW/m²

Figure 6. Surface temperature gradients for all heat sink geometries at velocity 1.8m/s, Pin = 40W

Figure 5. Surface temperature gradients for all heat sink geometries at velocity 2.4 m/s, Pin= 40W

Figure 7. Shows the impact of the five shapes of the heat sinks on the Nusselt number with varying heat fluxes. The velocity of air is (2.4m/s). As seen in the figure the Nusselt number is the maximum value with a circular cut with a gradual increase of the heat fluxes.

Figure 8. illustrates the relationship between the Nusselt number and heat transmission coefficient. When the coefficient of heat transmission increases, the Nusselt number rises. **CCFs** indicate the most outstanding value in comparison to different shapes of heat sinks.

Figure 9 depicts the effect of mass flow rate on thermal resistance for all investigated HSs. This graph demonstrates that flow fragmentation significantly reduces thermal resistance, resulting in enhanced thermal performance. Compared to traditional HSs, the thermal resistance decreases by roughly 17.53% and 8.02% for **CFs** and **CCFs**, respectively, at greater flow rates. Inversely proportional to the thermal resistance, the thermal resistance decreases as the flow rate increases (reduced average surface temperature). Additionally, **CCFs** have a lower thermal resistance than other cases for all mass flow rates considered.
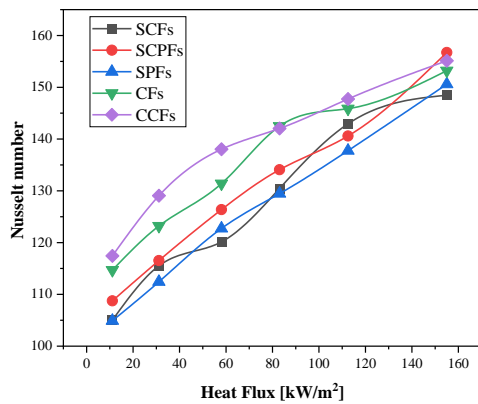
Figure 7. Distribution of Nusselt number with different heat fluxes for all heat sinks
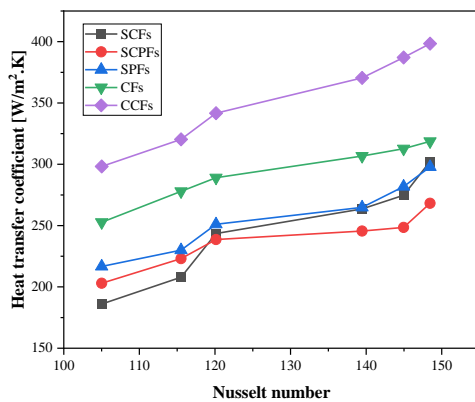

Figure 8. Distribution of Nusselt with heat transfer coefficient for all cases study
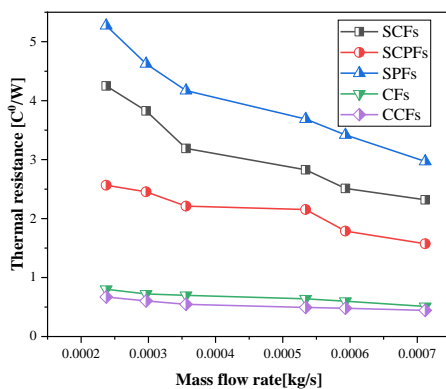

Figure 9. Distribution of Thermal Resistance with different mass flow rates for all heat sinks

5. Conclusions

In this study, numerical simulation was used to improve the thermal performance of the different types of a heat sinks and suggest circular and circular cut fins as a new design in addition to other conventional configurations. Simulations have been performed using CFD COMSOL 5.6 software for Reynolds numbers in the hydraulic diameter ranging from 2418 to1591. The obtained results indicate that the circular and circular cut provided the best thermal performance better than the other configurations. In addition, the heat transfer coefficient and Nusselt number rise for all heat sink when heat flux and Reynolds number increase. Furthermore, the average Nusselt number was (155, and153) for **CCFs** and **CFs** respectively Therefore, for each heat sink, the thermal resistance falls as the heat flow and Reynolds number rise. The heat sink with a circular cut has the highest heat transfer coefficient and the lowest thermal resistance.

REFERENCES

[1] Nilpueng, K., et al., *Effect of pin fin configuration on the thermal performance of plate pin fin heat sinks.* Case Studies in Thermal Engineering, 2021. **27**: p. 101269.

[2] Ahmadian-Elmi, M., et al., *A comprehensive study on parametric optimization of the pin-fin heat sink to improve its thermal and hydraulic characteristics.* International Journal of Heat and Mass Transfer, 2021. **180**: p. 121797.

[3] Chingulpitak, S., et al., *Experimental and numerical investigations of heat transfer and flow characteristics of cross-cut heat sinks.* International Journal of Heat and Mass Transfer, 2016. **102**: p. 142-153.

[4] Huang, C.-H. and Y.-H. Chen, *An impingement heat sink module design problem in determining simultaneously the optimal non-uniform fin widths and heights.* International Journal of Heat and Mass Transfer, 2014. **73**: p. 627-633.

[5] Huang, C.-H. and Y.-H. Chen, *An optimal design problem in determining non-uniform fin heights and widths for an impingement heat sink module.* Applied thermal engineering, 2014. **63**(2): p. 481-494.

[6] Shadlaghani, A., et al., *Optimization of triangular fins with/without longitudinal perforate for thermal performance enhancement.* Journal of Mechanical Science and Technology, 2016. **30**(4): p. 1903-1910.

[7] Nilpueng, K., et al., *Heat transfer and flow characteristics of the sinusoidal wavy plate-fin heat sink with and without crosscut flow control.* International Journal of Heat and Mass Transfer, 2019. **137**: p. 565-572.

[8] Freegan, B., et al., *CFD analysis of heat transfer enhancement in plate-fin heat sinks with fillet profile: Investigation of new designs.* Thermal Science and Engineering Progress, 2020. **17**: p. 100458.

[9] Sertkaya, A.A., M. Ozdemir, and E. Canli, *Effects of pin fin height, spacing and orientation to natural convection heat transfer for inline pin fin and plate heat sinks by experimental investigation.* International Journal of Heat and Mass Transfer, 2021. **177**: p. 121527.

[10] Altun, A.H. and O. Ziylan, *Experimental investigation of the effects of horizontally oriented vertical sinusoidal wavy fins on heat transfer performance in case of natural convection.* International Journal of Heat and Mass Transfer, 2019. **139**: p. 425-431.

[11] Feng, S., et al., *Natural convection in a cross-fin heat sink.* Applied Thermal Engineering, 2018. **132**: p. 30-37.

[12] Pathak, K.K., A. Giri, and B. Das, *Thermal performance of heat sinks with variable and constant heights: An extended study.* International Journal of Heat and Mass Transfer, 2020. **146**: p. 118916.

[13] Moradikazerouni, A., et al., *Investigation of a computer CPU heat sink under laminar forced convection using a structural stability method.* International Journal of Heat and Mass Transfer, 2019. **134**: p. 1218-1226.

[14] Yousfi, A., D. Sahel, and M. Mellal, *Effects of A Pyramidal Pin Fins on CPU Heat Sink Performances.* Journal of Advanced Research in Fluid Mechanics and Thermal Sciences, 2019. **63**(2): p. 260-273.

[15] Tariq, A., et al., *Comparative numerical and experimental analysis of thermal*

and hydraulic performance of improved plate fin heat sinks. Applied Thermal Engineering, 2021. **182**: p. 115949.

[16] Razavi, S., B. Osanloo, and R. Sajedi, *Application of splitter plate on the modification of hydro-thermal behavior of PPFHS.* Applied Thermal Engineering, 2015. **80**: p. 97-108.

[17] Usman, H., et al., *An experimental study of PCM based finned and un-finned heat sinks for passive cooling of electronics.* Heat and Mass Transfer, 2018. **54**(12): p. 3587-3598.

[18] Bahiraei, M., et al., *CFD analysis of employing a novel ecofriendly nanofluid in a miniature pin fin heat sink for cooling of electronic components: Effect of different configurations.* Advanced Powder Technology, 2019. **30**(11): p. 2503-2516.

[19] Alhusseny, A., et al., *Dissipating the heat generated in high-performance electronics using graphitic foam heat-sinks cooled with a dielectric liquid.* International Communications in Heat and Mass Transfer, 2021. **127**: p. 105478.

[20] Jilte, R., et al., *Cooling performance of a novel circulatory flow concentric multi-channel heat sink with nanofluids.* Nanomaterials, 2020. **10**(4): p. 647.

[21] Jaffal, H.M., H.S. Jebur, and A.A. Hussein, *Numerical and experimental investigations on the performance characteristics for different shapes pin fin heat sink.* IJOCAAS, 2018. **4**(3): p. 330-343.